Macromolecules

Article

pubs.acs.org/Macromolecules

New Experiments for Improved Theoretical Description of Nonlinear Rheology of Entangled Polymers†

Shi-Qing Wang,* Yangyang Wang, Shiwang Cheng, Xin Li, Xiangyang Zhu, and Hao Sun

Maurice Morton Institute of Polymer Science and Engineering, University of Akron, Akron, Ohio 44325, United States

ABSTRACT: The present work discusses four types of new experiments that can improve the current theoretical description of nonlinear rheology of entangled polymers. First, a slowly imposed strain is found to result in nonmonotonic evolution of the state of chain entanglement during quiescent relaxation, consistent with the idea of chain disentanglement after step shear. Second, the stress relaxation upon a sizable step strain is found to be identical to that for small step strain, consistent with a molecular scenario that a strained entangled melt has an entropic barrier to resist chain retraction. Third, the ability of a step-strained polymer to undergo elastic recovery is found to be the same up to strain amplitude of unity, and a sample sheared for a period much longer than the Rouse time is shown to still undergo nearly full elastic recovery. Fourth, an entangled melt, stretched at a rate significantly lower than the Rouse relaxation rate, undergoes full elastic recovery until the point of tensile force maximum. We have discussed an alternative conceptual framework to describe these nonlinear responses of entangled polymers despite the possibility that the tube model might be further remedied to characterize the new rheometric measurements presented in this work.

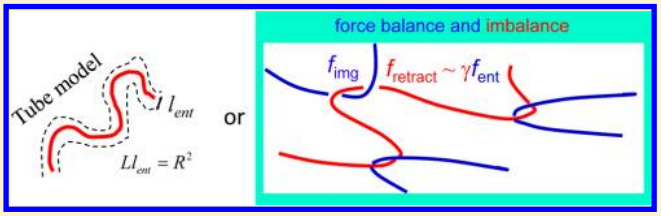

I. INTRODUCTION

Viscoelastic properties of entangled solutions and melts have been an important research area in polymer science and engineering. The subject of polymer dynamics is universal in the sense that it applies to all species with different chemical structures because it deals with polymers in their disordered liquid state. Research on rheology of entangled polymers intensified ever since 40 years ago when de Gennes opened a new era in polymer physics with the idea of *reptation*, envisioning a probe chain to perform snake-like motions in a cross-linked polymeric gel.[1] This notion was subsequently developed by Doi and Edwards into a tube model in a series of four seminal publications.[2−5] In the tube model, interchain excluded volume effects are treated by the insightful idea of Edwards[6] who perceived an impenetrable tube to mimic the constraint due to the chain uncrossability. Today, the reptation/tube theory offers a familiar depiction of chain diffusion and relaxation as well as nonlinear rheology of entangled polymers. Its appeal has a great deal to do with how the theory simplifies the extraordinarily complex many-body system into something tractable and comprehensible. Its successes and merits arise from the apparent agreement between some experiments and key aspects of the theory. On the 40th anniversary of the reptation idea, it is appropriate to study its major beneficiary, the tube model, in light of an emerging experimental background. To appreciate the apparent successes of the tube model, it is helpful to first mention the prior attempts.

Earlier efforts to describe rheological properties of entangled polymers and other viscoelastic materials was dominated by attempts to search for suitable constitutive equations based on continuum mechanics principles.[7−11] Like the Maxwell model, the various constitutive models including the K-BKZ model[12,13] all have parameters that are constant in space and time. Today, various constitutive models are still popularly employed in finite-element numerical computations to treat entangled polymeric liquids as smooth continua.

A large fraction of the constitutive models grew out of modification of the successful rubber elasticity theory[14] that is also known as the neo-Hookean network model in the rheology literature, where the zeroth order picture is to simply evaluate the observable stress in terms of the entropic changes associated with the deformation of all Gaussian strands between chemical cross-links. By allowing the "cross-links" to have finite lifetimes, transient network models[15−17] (TNM) emerges in 1950s to offer a phenomenological account of the role played by intermolecular interactions in noncross-linked polymeric liquids. In order to explain such nonlinear and non-Newtonian behavior as shear thinning, TNM allowed the junction lifetimes to depend on the applied rate in some phenomenological manner. Consequently, they are not a first-principles description of polymer rheology.

The tube model is also phenomenological rather than first-principles-based in the sense that the intermolecular interactions are modeled by restricting a test chain to tube-like confinement. It gained popularity because such key experimental features as *stress overshoot* upon startup shear (defined in the following Figure 1) and *strain softening* upon large step strain emerge automatically from the tube model. Another appealing character of the Doi−Edwards tube theory is

Received: February 28, 2012
Revised: March 30, 2013
Published: April 12, 2013

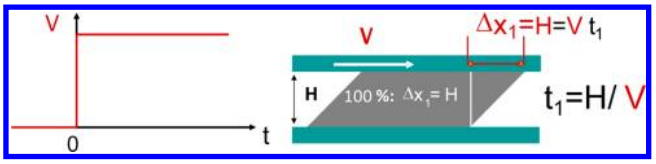

Figure 1. Depiction of startup shear at a nominal shear rate of $\dot{\gamma} = V/H$, for which, the time required to produce the first 100% of shear deformation is given by $t_1 = H/V = 1/\dot{\gamma}$.

that its integral form is similar to the phenomenological K-BKZ model[12,13] as if the tube theory has provided a molecular-level justification of the K-BKZ model.

All integral-form constitutive models including the Lodge network theory model,[18] the K-BKZ model, and the Doi–Edwards (DE) tube model, have two common features. (A) The constitutive equation involves the spectrum of *equilibrium* relaxation times. (B) There is a memory function in the integral for the stress tensor to indicate that the stress constantly arises from recoverable deformation over a period of time in the past prescribed by the equilibrium relaxation spectrum. Since the origin of stress should be entirely intermolecular in steady flow, a realistic molecular model has to treat the interchain interactions explicitly. The DE model represented the intermolecular interactions in terms of a tube and evaluated the stress from the intrachain forces.

This paper is organized as follows. In section II, we examine the structure of the tube theory in terms of its construction and discuss an alternative framework derived from the emerging phenomenology. Section III details the basic features of the tube theory that are intimately related to its starting assumptions. In section IV we describe various experimental data that are consistent with the alternative ideas before concluding in section V.

Before making a comparison between the two different standpoints, we introduce the basic notations and define the conditions for nonlinear rheology of entangled polymers.

The Maxwell model identifies an essential property of viscoelastic materials: a dominant relaxation time τ_0, also known as the terminal relaxation time or reptation time for entangled polymers (using the tube model language). Borrowing the idea of Maxwell, linear response of viscoelastic materials is expected when the external deformation is either small or taking place sufficiently slowly. Taking startup simple shear deformation with rate $\dot{\gamma} = V/H$ for example, Figure 1 shows that $t_1 = H/V = 1/\dot{\gamma}$ is the time required to produce one unit of shear strain. Weissenberg introduced a dimensionless number, $Wi = \tau_0/t_1 = \dot{\gamma}\tau_0$, to parametrize how fast the applied shear is. The degree of the initial elastic deformation is upper bounded by Wi. This measure can be straightforwardly extended to other modes of deformation such as uniaxial extension at a Hencky strain rate $\dot{\varepsilon}$ so that $Wi = \dot{\varepsilon}\,\tau_0$. When $Wi \ll 1$, there is negligible elastic deformation, and the external deformation does not alter the state of chain entanglement. Therefore, the condition of $Wi \ll 1$ ensures linear response, where the theoretical description of entangled polymeric liquids can avoid the challenge of dealing with any non-equilibrium state of chain entanglement. When $Wi \gg 1$, linear response is possible only if the imposed strain does not exceed a critical level, which can be identified empirically. For entangled polymer solutions and melts in simple shear, this critical strain is known to be on the order of unity.

Upon a startup deformation with $Wi \gg 1$, the key question is what happens when the external strain grows continuously. Do we expect the mechanical response to be solid-like up to $t \sim \tau_0$, corresponding to a strain of $Wi \gg 1$? When does the "solid" turn into a "liquid"? In other words, when is the structure of the chain entanglement network irreversibly altered? Before an entangled polymer suffers irrecoverable deformation, we can expect nearly full elastic recovery upon letting go stress free. Thus, a special point of interest is the moment when the system loses its ability to have full elastic recovery.

II. CONTRASTING TWO DIFFERENT PICTURES

It is universally accepted that the chain entanglement arises from the uncrossability, which is due to a combination of excluded volume and chain connectivity. The packing model[19−22] conjectured about the onset of chain entanglement at a critical degree of molecular crowdedness, expressing the entanglement molecular weight M_e in terms of the packing length p. But it offers no clue about how to depict the spatial molecular arrangement, e.g., mutual interpenetration, dynamically.

Arthur Lodge pointed out[23] in 1989 that there are two fundamentally different kinds of theoretical treatment for entangled polymers in terms of, either "strong, localized interactions of the network junction type", or "smoothed-out, uniform interactions representing a mean field". The former recognizes the explicit role of intermolecular coupling at the entanglement points and asserts that entangled polymeric liquids are network-like, involving many-body interactions. The tube model is obviously the latter type because it treats intermolecular interactions in a smoothed-out, uniform way by representing a test chain in an imaginary tube. Since it cannot keep track of the original entanglement structure, it cannot perceive how the initial state of entanglement becomes updated and renewed in presence of external deformation. Below we review two different pictures concerning chain entanglement in presence of external deformation.

1. Structure of the Tube Model. The tube model has been widely accepted and extensively applied as the standard model in polymer rheology. In other words, it is the prevailing theoretical description known to all workers in the field. Here and below "the tube model" refers to any version of the tube theories[24,25] including the latest[26] unless specified otherwise. On the other hand, by "Doi–Edwards tube model", we refer to the version established by their first four papers.[2−5] It is important to first understand how the tube model was constructed and how its foundation may be tested by experiment.

To make a mathematical description of polymer chain entanglement is a formidably challenging task, let alone depicting analytically how the entanglement behaves under large fast external deformation. The objective of the tube model is not to depict chain entanglement since it does not and cannot delineate the origin of chain entanglement. Instead, the tube model attempts to depict the consequence of entanglement for polymer dynamics. Specifically, inspired by the success of the classical rubber elasticity theory,[14] the construction of the tube model is based on the following three hypothetical elements, simplifying the task to describe the many-body system in terms of a single-chain picture. (i) The experimentally measured stress is of intrachain origin. Moreover, (ii) the effects of surrounding chains on a test chain are to provide a tube-like invisible constraint so that the transverse

dx.doi.org/10.1021/ma300398x | *Macromolecules* 2013, 46, 3147−3159

degree of freedom is limited to a narrow space known as the tube diameter. In the linear response regime, the entanglement network is always in equilibrium, and an explicit account of the intermolecular interactions may be unnecessary. In other words, it may be adequate to approximate the physics of polymer dynamics by erecting an infinitely high confinement barrier for a test chain. In the nonlinear response regime, the tube model has an inevitable outcome that can be reviewed as its third assumption: (iii) The test chain undergoes Rouse dynamics inside the tube so that there would be barrier-free chain retraction at Rouse time τ_R upon affine deformation of the tube. In terms of τ_R, the product $\dot{\gamma}\tau_R$ or $\dot{\varepsilon}\tau_R = Wi_R$ will be called the Rouse−Weissenberg number in this paper. When the deformation is carried out at $Wi_R \ll 1$, the chain retraction would recover the equilibrium contour length, and affine deformation ceases beyond $t = \tau_R$ according to the tube model. In absence of chain stretching for $Wi_R < 1$, chain orientation alone contributes to the stress. Consequently, the tube model interprets the stress overshoot during startup shear with $Wi_R < 1$ as merely due to progressive chain orientation.

Because the tube model represents polymer entanglement in terms of a smoothed-out, uniform confinement in a true mean-field manner and is not based on consideration of forces, it cannot determine how the state of entanglement is altered and renewed. Since the transverse constraint is always there, a tube always exists to surround the test chain regardless whether the chain retracts or not. In other words, it is challenging for the tube model to describe how chain disentanglement may occur during fast large external deformation.

2. A Dynamic Network Picture. Recently, a great deal of new information has begun to indicate that for $Wi > 1$ entangled polymers may have to be regarded as a network formed by localized intermolecular interactions. In the new network picture,[27] we perceive polymer entanglement as depicted in Figure 2 where an entanglement strand from the

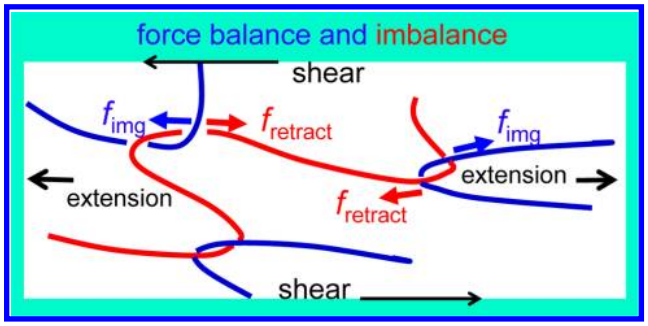

Figure 2. A cartoon to depict an entangled polymer in terms of a network-like picture. It shows a strand between entanglements that is strained either in shear to γ or extension to λ. The elastic retraction force $f_{retract}$ ($\sim \gamma f_{ent}$ for simple shear and $\sim (\lambda - 1/\lambda^2) f_{ent}$ for uniaxial extension) originates from the molecular deformation that occurs in absence of chain sliding at the entanglement points because of the intermolecular gripping force f_{im} (IGF).

test chain (in red online) is anchored at two hairpins and displaced by the surrounding (blue) chains during external deformation. Thus, upon startup deformation with $Wi_R > 1$, the intermolecular gripping forces f_{img} (IGF) is believed arise due to the chain uncrossability associated with the excluded volume effect on *slowly* moving/sliding chains.[28] When the external deformation displaces chains in opposing directions, the uncrossability produces the IGF, which in turn causes chain deformation, leading to the buildup of intrachain elastic retraction force $f_{retract}$. The original entanglements are lost in a massive amount when the elastic retraction force $f_{retract}$ within the strand reaches the intermolecular gripping forces f_{img} (IGF), i.e., $f_{retract} \sim f_{img}$.[29,30] Subsequently the test chain begins to slide past other chains at the entanglement points as shown in Figure 2. This event leads to the stress decline since a large fraction of chains in the entanglement network should undergo such chain sliding. In other words, in our picture, the stress overshoot during startup shear is a consequence of molecular chain disentanglement, in contrast to the tube-model picture of the chain orientation.

The rate of deformation, relatively to the chain relaxation rate, determines how effectively the chain uncrossability produces the IGF because the externally driven displacement has to compete with the chain relaxation dynamics. For $Wi < 1$, the displacement is so slow that the chains readily reptate past one another, without becoming appreciably deformed. In other words, IGF is obviously inactive for $Wi < 1$. Although we are currently unable to derive the IGF by formulating an analytical treatment of the topological Gaussian chain network under external deformation, the existence and characteristics of the IGF seem obvious to us. Others may view it as a hypothetical force whose origin is physical hinderance.

During startup deformation, in the limit of affine deformation, the stress grows monotonically with the imposed strain. For simple shear, shear stress $\sigma = G_{pl}\,\gamma$, and for uniaxial extension the engineering stress $\sigma_{engr} = G_{pl}(\lambda - 1/\lambda^2)$, where G_{pl} is the elastic plateau modulus associated with the entanglement network. According to the rubber elasticity theory, the stress arises from the intrachain elastic retraction force $f_{retract}$. The current authors propose[29] that the areal number density of entanglement strands ψ is related to G_{pl} as $G_{pl} = \psi f_{ent}$, where $f_{ent} \sim k_B T/l_{ent}$ is the entanglement force associated with the entropic barrier that provides the structural integrity or cohesion of the entanglement network on time scales shorter than τ_0, with l_{ent} being the entanglement spacing. Therefore, equating $\psi f_{retract}$ to σ for simple shear and to σ_{engr} for uniaxial extension, we have $f_{retract} = \gamma f_{ent}$ for simple shear and $(\lambda - 1/\lambda^2) f_{ent}$ for uniaxial extension. During the startup deformation, the increase of $f_{retract}$ with shear strain γ or stretching ratio λ cannot continue without bound because f_{img} is of a finite magnitude. Thus, the force imbalance must occur, and the accompanying chain sliding at the entanglement points is the molecular mechanism for the observed macroscopic nonlinearity either during startup deformation or after a large stepwise strain.

Experimental data suggest that f_{img} is comparable to f_{ent} for the applied rate between $Wi > 1$ and $Wi_R < 1$,[31,32] because the molecular "yielding" by chain disentanglement usually occurs at a modest strain. In other words, for $Wi > 1$ and $Wi_R < 1$, the strain γ_{max} at the stress overshoot is only around two so that the magnitude of $f_{retract}$ at the stress overshoot is on the same order as f_{ent}. For example, for rates satisfying $Wi_R < 1$, the strain γ_{max} at the stress overshoot is only around two.[31] In this limit, the uniaxial extension terminates with rupture-like failure, which was interpreted as evidence that the IGF is unimportant in this regime.[32] Conversely, the IGF appears dominant and grows strongly with the deformation rate for $Wi_R > 1$ because γ_{max} grows with Wi_R, reaching as high as ten, implying that there is considerable f_{img} to balance $f_{retract} > 10 f_{ent}$.

The use of "yielding" to describe such nonlinear responses as stress overshoot is hard to find in the literature on melt

dx.doi.org/10.1021/ma300398x | *Macromolecules* 2013, 46, 3147−3159

rheology of entangled polymers. Here and through the text, we use this terminology in a crude phenomenological sense to convey the notion that irreversible deformation must replace the initial elastic recoverable deformation during continuous external deformation. The experimental signature of macroscopic yielding, i.e., transition from the initial elastic deformation to the irrecoverable deformation upon startup simple shear or uniaxial extension, is interpreted to be the emergence of a shear or engineering stress overshoot (i.e., maximum) at γ_{max} or λ_{max}. It is in this phenomenological sense that Matsuoka used the phrase "yielding" to anticipate the response of polymer melts upon startup of continuous deformation in his monograph:[33] See pp 180 and 194 for some relevant statements. The "yielding" is frequently used in solid mechanics of metallic, colloidal and polymeric glasses, gels, dense suspensions, semicrystalline polymers, granular materials, etc. In the solid mechanics of these materials, the concept of yield is sometimes associated with the material failure that occurs by strain localization. For glasses, yielding is a common term to describe loss of solid-like response: Stress builds upon continuous external deformation that produces a state where the rate of structural relaxation increases many orders of magnitude to approach the rate of external deformation.[34] This event of plasticity is clearly a flow state because structural changes have to occur on the time scale of the reciprocal deformation rate. There is also the concept of yield-stress for materials that are solid-like at rest, possessing relaxation times too long relative to the experimental time scale, but can be made to flow beyond a certain stress level.

Unlike these solid-like materials where the concept of yielding has been routinely invoked,[35] entangled polymer solutions and melts have a terminal flow regime accessible for $Wi < 1$. Because of the existence of this readily observable flow zone in entangled polymer solutions and melts, unlike the yield-stress materials, the researchers in the field did not regard such features as the stress overshoot to be a sign of yielding, even though such a transition clearly exists upon startup deformation. With $Wi > 1$, entangled polymers are forced to yield (in the above sense) on time scales shorter than τ_0 at the shear stress maximum during startup shear, for example. On the basis of Figure 2, we have offered a molecular mechanism for this yielding: It occurs upon the force imbalance as discussed above in Figure 2 and involves the chain disentanglement. In passing, it is important to note that macroscopic yielding does not have to result in strain localization. For many viscoelastic materials including modestly entangled polymers[36,37] where the nonyielded state is not greatly different from the yielded state in terms of their mechanical characteristics, the transition from elastic deformation to flow can take place homogeneously.

Chain disentanglement upon force imbalance can also be induced by a sudden termination of the external deformation. In absence of continuing displacement, IGF is considered to be no longer active[28] against the intrachain elastic retraction force. If there has been sufficient retractive force such as the case of sudden of large stepwise deformation produced with $Wi \gg 1$, chain sliding is inevitable because the high level of $f_{retract}$ ($>f_{ent}$) can overcome the entropic barrier quantified by the entanglement force f_{ent}. When the stepwise strain is small enough, the resulting $f_{retract}$ is lower than f_{ent} so that no force imbalance and molecular yielding can occur.

When the system is sufficiently entangled,[38] a step-strained entangled polymer solution[39] or melt[40] undergoes nonquiescent relaxation, due to the localized breakup of the entanglement network.[41] Prior to our reports,[39,40] it was usually perceived that a step strain could only result in quiescent stress relaxation although there has been a suggestion of instabilities in stress relaxation.[42] Thus, the observations of macroscopic motions after a sizable stepwise strain of either shear[39,40] or extension[43,44] were clearly alarming. It even takes place for $Wi_R < 1$ although there would be no chain stretching according to the tube model.[40] Such elastic yielding occurs whenever the stepwise strain is sufficiently large, e.g., when $\gamma > 1$ involving step shear or $(\lambda - 1/\lambda^2) > 1$ involving step extension.

III. KEY ELEMENTS OF THE TUBE THEORY

In this section, we review the predictions and molecular pictures associated with the tube theory by examining the model's foundation and structure.

1. Barrier-Free Chain Retraction on the Rouse Time Scale. The tube model assumes that upon startup of external straining with $Wi > 1$ affine deformation of the tube occurs until the test chain inevitably retracts within the tube on the Rouse time τ_R. The test chain has only frictional interactions with the imaginary tube and encounters no entropic barrier. This construction separates the molecular deformation into chain stretching and orientation respectively, decoupling the orientation dynamics from with the chain stretching dynamics. Three specific consequences follow from this barrier-free chain retraction:

A. Spontaneous Stress Decline at τ_R for $Wi_R > 1$. Appreciable chain retraction is expected to occur for *any level* of imposed step strain produced with $Wi_R > 1$. Specifically, this process is expected to produce a measurable stress decline for a step strain with moderate amplitude $\gamma_0 < 1$ (simple shear) and $\lambda < 2$ (uniaxial extension). Here we show how the tube model describes the effect of chain retraction on stress relaxation after a large step strain.[45] Eq 7.123 in the Doi–Edwards book[46] gives

$$\sigma_{\alpha\beta} = Q_{\alpha\beta}(\mathbf{E})\{1 + [\alpha(\mathbf{E}) - 1]\exp(-t/\tau_R)\}^2 G_{eq}(t) \quad (1a)$$

where the tensorial orientation function Q and stretching factor α each respectively depend on the type of the deformation field $\mathbf{E}$, and G_{eq} is the equilibrium relaxation modulus. Note that the function Q in this paper differs from that in the DE book by a factor of 4/15. The consequence of the barrier-free chain retraction is a decline in the stress as the time-dependent factor represented by $\{\ \}^2$ of eq 1a decreases from α^2 at $t = 0$ to 1 when $\exp(-t/\tau_R) \ll 1$. Here we only need to include the longest Rouse time in the curled brackets to capture the effect of chain retraction on the time-dependent stress. The stretching factor α can be readily computed. For simple shear, we have

$$\alpha(\mathbf{E}) = \langle(1 + 2\gamma u_x u_y + \gamma^2 u_y^2)^{1/2}\rangle = \left(\frac{1}{\pi}\right)\int_0^\pi d\phi \int_0^1 dx \sqrt{1 + (1 - x^2)(\gamma \sin 2\phi + \gamma^2 \sin^2\phi)} \quad (1b)$$

where $\langle\ \rangle$ is the average over the isotropic (equilibrium) state, and the last expression can be evaluated numerically. For uniaxial extension, we can get a closed form for the stretching factor

dx.doi.org/10.1021/ma300398x | Macromolecules 2013, 46, 3147–3159

$$\alpha(\mathbf{E}) = \langle[\lambda^2 u_z^{\,2} + (u_x^{\,2} + u_y^{\,2})/\lambda]^{1/2}\rangle$$
$$= \int_0^1 dx\, \sqrt{x^2\lambda^2 + (1-x^2)/\lambda}$$
$$= \frac{1}{2}\left[\lambda + \frac{1}{\sqrt{\lambda(\lambda^3-1)}} \ln(\lambda^{3/2} + \sqrt{\lambda^3 - 1})\right] \quad (1c)$$

Figure 3 shows how α^2 varies with the step strain amplitude respectively for both step shear of amplitude γ and uniaxial

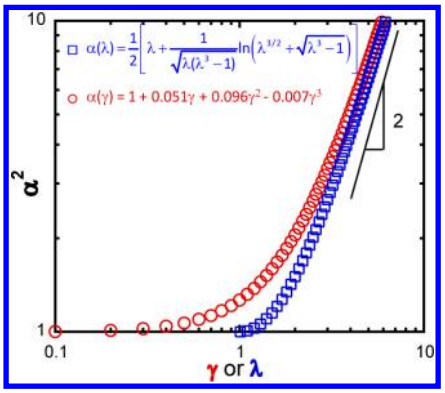

Figure 3. The square of the stretching factor, either $\alpha(\gamma)$ for simple shear or $\alpha(\lambda)$ for uniaxial extension, is plotted as a function of the imposed shear strain γ or stretching ratio λ. Here the functional form of $\alpha(\gamma)$ can be matched with a polynomial. In both cases, at modest deformations, e.g., below $\gamma = 1$ and $\lambda = 2$, α^2 is discernibly above unity so that a stress drop in magnitude of $(\alpha^2 - 1)$ is experimentally measurable.

extension with stretching ratio $\lambda = L/L_0$ (L_0 being the original sample length). Specifically, for simple shear, $\alpha^2(\gamma = 0.7) \cong 1.13$. In the case of uniaxial extension, $\alpha^2(\lambda = 1.5) \cong 1.15$.

B. Stress Overshoot and Nonmonotonicity from Orientation for $Wi_R \ll 1$. The Doi–Edwards tube model states that "the stress is mainly due to the intramolecular entropic force; the intermolecular force acts primarily to keep the volume of the system constant and is not important for the anisotropic part of the stress."[3] Consider the condition of a startup deformation with $Wi_R \ll 1$ and $Wi > 1$. Because of the chain retraction, a test chain undergoes little stretching in the sense that the affine deformation only lasts over a period comparable to τ_R, corresponding to a strain equal to $Wi_R \ll 1$. In absence of chain stretching, the shear stress arises entirely from the chain orientation during startup shear according to

$$\sigma_{xy}(\dot\gamma, t) = G_{pl}\int_{-L/2}^{L/2} d(s/L)\,\langle u_x(s,t)u_y(s,t)\rangle$$
$$= G_{pl}\int_0^t dt'\,\mu(t')Q_{xy}(\dot\gamma t') \quad (2)$$

where the first equality is eq 7.178 of ref 46 or eq 1.2 of paper 4 of Doi–Edwards,[2] and the second equality arises from the averaging $\langle\ \rangle$ under the condition that the primitive chain segmental vector $\boldsymbol{u}$ could orient affinely upon a startup shear at rate $\dot\gamma$. Here G_{pl} is the elastic plateau modulus, μ is a memory function involving the full *equilibrium* relaxation spectrum $\{\tau_p\}$, with $\tau_p = \tau_0/p^2$, and $Q_{xy}(x)$ is the orientation function whose mathematical form can be approximated by $Q_{xy}(x) \simeq x/(1 + x^2/5)$. This nonmonotonic function Q_{xy} indicates that when the elapsed strain $\gamma = \dot\gamma t$ is beyond $\gamma_{max} = \sqrt{5} = 2.24$, the excessive chain orientation results in a lower shear stress. In other words, σ_{xy} reaches a maximum $\sigma_{max} = 1.1\ G_{pl}$ around $\gamma_{max} = \sqrt{5} = 2.24$, as depicted in Figure 4. Thus, the tube model interprets the experimentally observed stress overshoot as merely due to the continuing chain orientation.

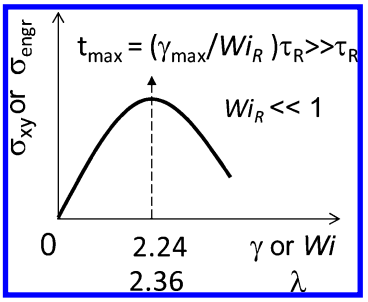

Figure 4. Shear stress σ_{xy} or engineering stress σ_{engr} as a function of imposed strain for either simple shear (γ) or uniaxial startup deformation (λ) under the condition of $Wi_R \ll 1$ and $Wi > 1$, where the peak emerges just above two in either mode of deformation (γ or λ). For the case of shear, according to the tube model, the curve is quantitatively given by the orientatioal function $Q_{xy}(x)$ given below eq 2, where x can be either $\gamma = \dot\gamma t$ to depict overshoot during startup shear or Wi to indicate stress nonmonotonicity in steady shear. The curve is also the Doi–Edwards damping function for the stress at long times.

Similarly, under the condition of $Wi_R \ll 1$, the Doi–Edwards tube model also evaluated the mechanical response of an entanglement network to startup uniaxial extension.[5] Since the chains retract without stretching, the number of load-bearing entanglement strands per unit cross-sectional area stays constant during the startup extension as depicted in Figure 5a. When chain stretching is negligible for $Wi_R \ll 1$, the Cauchy (true) stress σ arises from chain orientation alone and actually levels off, i.e., $\sigma \sim \sigma_\infty$ = constant after sufficient straining so that the engineering stress $\sigma_{engr} = \sigma/\lambda$ declines with λ as shown in Figure 4. This tensile force decline beyond $\lambda_{max} = 2.36$ in the tube model arises from the shrinkage of the cross-sectional area, not from any cohesive breakdown of the

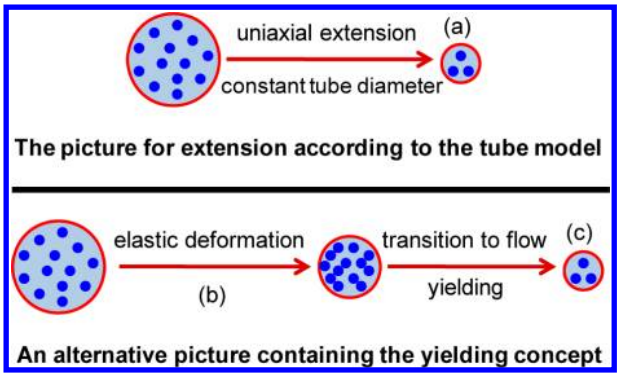

Figure 5. In part a, as stretching continues (i.e., stretching ratio λ increases), the number of entanglement strands in the specimen decreases in proportion to the area reduction: $A/A_0 = 1/\lambda$. This is the picture in the Doi–Edwards model for startup extensional deformation with $Wi_R \ll 1$. An alternative view shows how the number of load-bearing entanglement strands in the entire cross-section of the system remains nearly constant during initial elastic deformation in part b and only show significant decrease upon the molecular yielding as depicted in part c.

dx.doi.org/10.1021/ma300398x | Macromolecules 2013, 46, 3147–3159

entanglement network. In our picture, the affine network deformation (leading to a geometric condensation of the entanglement strands) as depicted in Figure 5b occur first, and yielding involves the step depicted in Figure 5c.

Additionally, in steady state, the σ_{xy} vs $\dot{\gamma}$ curve is given by $\sigma_{xy} \simeq G_{pl}Q_{xy}(Wi)$, displaying a maximum at $Wi = \dot{\gamma}\tau_0 \sim \sqrt{5} = 2.24$ as shown in Figure 4. This nonmonotonicity again stems merely from the excessive chain orientation because the tube model considers the mechanical stress to be of intrachain origin. In reality, the steady-state stress must have intermolecular contributions. In other words, there is no proof that intrachain contributions already incorporate the interchain component of the stress. Nevertheless, such a nonmonotonic character has been repeatedly taken as the mechanism for shear banding.[47−49] We will return in a subsequent section to comment on whether or not such nonmonotonicity is relevant to the experimental observation of shear banding.[38,50,51]

C. Nonaffine Deformation and Lack of Elastic Recovery for $Wi_R \ll 1$. Startup deformation with $Wi > 1$ and $Wi_R \ll 1$ is essentially nonaffine because of the chain retraction on the Rouse time scale. Consequently, elastic recovery should be negligible relative to a finite strain of, say, unity that takes a time of $t_1 = 1/\dot{\gamma}$ or $1/\dot{\varepsilon} = \tau_R/Wi_R \gg \tau_R$. Moreover, according to the tube model, the startup deformation with $Wi > 1$ and $Wi_R \ll 1$ only produces chain orientation. Upon cessation of the external deformation produced with $Wi_R \ll 1$, the tube model expects a monotonic recovery of the deformed state of chain entanglement toward the isotropic equilibrium state.

As the conclusion of this subsection, III.1, we point out that, among the three components of the tube model of Doi and Edwards listed in subsection II.1, the third (iii) that all chains undergoes barrier-free retraction on the Rouse time upon startup deformation can be most effectively tested by experiment. The chain retraction on the Rouse time scale during startup and stepwise deformation has the following consequences: (a) stress decline around τ_R due to chain retraction during stress relaxation from step strain made at $Wi_R > 1$; (b) lack of elastic recovery after one strain unit of stepwise deformation produced at $Wi_R \ll 1$; (c) nonmonotonicity the steady shear stress vs rate relation for $Wi > 1$; (d) a monotonic return of the state of chain entanglement after termination of a startup shear produced with $Wi_R \ll 1$, prior to the stress overshoot that occurs around $\gamma_{max} \sim 2$. The present work aims to design experiments that can test these consequences of the tube model.

2. Incorporation of Convective Constraint Release (CCR): A Revision of the Tube Model. The most well-known symptom (often regarded as the flaw) of the Doi−Edwards tube model is its prediction of the so-called stress maximum, i.e., the steady-state shear stress σ_{xy} declining with increasing applied shear rate $\dot{\gamma}$ just beyond $Wi = \sqrt{5}$, as shown in Figure 4. To remove this undesirable feature, it was proposed that the effect of convective constraint release (CCR)[52,53] be introduced to modify the relaxation dynamics and to remove the nonmonotonicity in the predicted flow curve of $\sigma_{xy} \sim Q_{xy}(Wi)$ in Figure 4. Specifically, under the condition of $Wi_R \ll 1$ and $Wi > 1$ in steady shear, an effective relaxation time τ_{eff} was proposed[53] to be of the form: $1/\tau_{eff} = 1/\tau_0 + A\dot{\gamma}$. Through the CCR, the stress maximum can be made to disappear. There are several newer versions[26,54,55] of the tube theory that treat chain retraction as one component of CCR to develop a self-consistent closure of the mean field approximation of the tube model for nonlinear rheology. The incorporation of CCR is based on kinematics, not on the basis of force evaluation. Consequently, such a modified tube model cannot prescribe *a priori* whether the nonmonotonicity should be absent or not.

For $Wi_R > 1$, the tube model envisions the shear stress decline after the overshoot during a startup shear to arise from a combination of chain retraction at the Rouse time τ_R and the CCR that modifies the relaxation rate to be comparable to the imposed rate. Since the CCR represents irreversible changes of the entanglement network it should not occur until the onset of chain mutual sliding upon the force imbalance, leading to "yielding" of the entanglement network. In other words, much of CCR logically should not occur before the stress overshoot. Moreover, our experimental data indicate (a) the stress overshoot could occur much earlier than τ_R and (b) γ_{max} scales like[31] $\gamma_{max} \sim \dot{\gamma}^{1/3}$ instead of $\gamma_{max} \sim \dot{\gamma}$ that is anticipated by the tube model,[56] although some literature data showed the exponent higher than 1/3.[57−59]

IV. KEY EXPERIMENTAL FINDINGS

Despite some recent publications that discussed the weakness of the tube model,[60−64] the foundation of the tube model, as represented by the three elements reviewed in the first paragraph of subsection II.1, has never been explicitly and thoroughly tested. In fact, most experimental studies appear to have been carried out to validate the tube model.[65] Our work breaks this tradition and focuses on a critical examination of the tube model.

1. Summary of Existing Experimental Findings. *A. Shear Banding Is Only Metastable.* Ever since the first report of shear inhomogeneity in startup shear of entangled polymer solutions,[50,51] it has been suggested that the Doi−Edwards tube model[2] contained a prediction for the experimental observations because it prescribed a nonmonotonic relationship between the shear stress and rate in steady state as discussed in subsection III.1.B. However, recent experiments show[66] that shear banding might be only metastable and not a steady state property. Specifically, occurrence of shear banding requires *startup* shear at high rates ($Wi \gg 1$). When the condition of $Wi \gg 1$ was gradually approached over a long period of time, e.g., through slow ramp-up of the applied rate, shear banding no longer occurred in the same system that exhibited shear banding during the sudden startup shear. In absence of the nonmonotonicity feature and any spatial variation of the shear stress along the velocity gradient direction, it is challenging for any existing constitutive model to depict the observed metastable shear banding.[67]

B. Nonquiescent Relaxation after Step Strain. One of the most remarkable particle-tracking velocimetric (PTV) observations[39,40] is the discovery of macroscopic motions after step strain[68] when it exceeds a critical strain about unity for simple shear and a Hencky strain around 0.7−0.8 for uniaxial extension.[43] The finding casts doubt on a large number[69] of favorable[70] and unfavorable[71−73] comparisons between the stress relaxation experiment and the damping function of the tube model. There is also the worst form of macroscopic motions when wall slip takes place.[74,75] Such macroscopic motions can produce strong strain softening. An earlier study[42] based on the free energy function of the tube model has offered an explanation for the ultrastrain-softening reported of step shear of 1,4-polybutadiene[74] that could have involved massive wall slip.[75,76] Since this study[42] is based on the tube model, its explanation of the ultrastrain softening in terms of an elastic instability has nothing in common with the alternative idea that

the strained entanglement network overcomes an entropic barrier to undergo decohesion as reviewed in subsection II.2. A recent numerical study[77] also applied a monotonic version of the tube model to depict nonquiescent relaxation. It did so by assuming that the step strain involved a visible stress gradient and arguing that the experiment could always involve such a stress gradient.

2. Further Experiments. In the remaining of this article, we focus on several new experiments to provide additional ingredients for the theoretical picture of the present authors that was briefly outlined in subsection II.2. These new experiments depart from the previous studies,[50,51] in one crucial way: While the past studies concentrated on the delineation of strain localization in both shear and extension, these new experiments involve no macroscopic deformational inhomogeneity because both startup deformation and step strain produces a uniform deformation field both during and after straining.

Specifically, four different rheometric measurements have been carried out to do the following:

1 Probe the state of chain entanglement during relaxation from an imposed strain produced at $Wi_R \ll 1$. According to the tube model, the strained sample should only heal monotonically toward its equilibrium state during relaxation.
2 Examine stress relaxation after a *moderate* step strain involving $Wi_R \gg 1$, for which the tube model anticipates measurable stress decline due to the barrier-free chain retraction.
3 Use elastic recovery measurements to determine the state of chain entanglement during startup shear and after step strain. When the duration of external deformation (with $Wi > 1$ and $Wi_R < 1$) well exceeds the Rouse time τ_R, the strained system should not undergo significant elastic recovery: According to the tube model, there is negligible affine deformation.
4 Elucidate the nature of the maximum in engineering stress σ_{engr} under the condition of $Wi_R \ll 1$ in startup uniaxial extension. The tube model assigns no structural significance to the maximum in σ_{engr}.[78]

Below we summarize the key results from these new experimental studies, which in combination with the results reviewed in the preceding subsection, should stimulate future theoretical work in nonlinear rheology of entangled polymers.

A. Experimental Details. A.1. Materials. Several samples were used to carry out the following experiments. To ensure homogeneous shear upon startup shear and quiescent relaxation after a finite amount of imposed strain,[79] we prepared a moderately entangled solution, i.e., a 5% 1,4-polybutadiene (PB) solution, made of monodisperse long chain with $M_w = 1.05 \times 10^3$ and $M_n = 1.01 \times 10^3$ kg/mol dissolved in a 1,4-polybutadiene matrix with $M_w = 10.5$ kg/mol and $M_n = 8.9$ kg/mol. This 1M5%-10K sample has 18 entanglements per chain, a terminal relaxation time of $\tau_0 = 19$ s and a Rouse time τ_R equal to 0.35 s. It was prepared by first dissolving the parent ultrahigh molecular weight polybutadiene in a mixture of the low MW polybutadiene solvent and toluene (cosolvent). Most of the toluene was evaporated slowly under a hood, and the rest was removed in a vacuum oven at room temperature. A second sample is a monodisperse entangled polymer melt, i.e., styrene–butadiene copolymer rubber (SBR) that has $Z = 33$ entanglements per chain, corresponding to $M_w = 161$ kg/mol and $M_e = 4.8$ kg/mol (25.6% styrene, 74.4% butadiene that has 70% vinyl). At $T = 30$ °C, the reptation time τ_0 of this melt is 1340 s and the Rouse time τ_R, estimated according to the two methods,[80] is around 13.4 s. The third sample is another SBR melt with $M_w = 241$ kg/mol and $M_e = 2.4$ kg/mol (21% styrene, 79% butadiene that has 40% vinyl) that has $Z = 98$ entanglements per chain, reptation time $\tau_0 = 34$ s and $\tau_R = 0.12$ s

A.2. Apparatuses. Two rotational rheometers were employed to carry out the designed experiments. The shear rheology experiments on the PB solution, to be described in sections IV.2.B and IV.2.D, were performed at 25 °C using the controlled-torque rheometer (Physica MCR301, Anton Paar USA) in a cone–plate assembly involving a 25 mm diameter and 2° cone angle. The elastic recoil tests involving uniaxial extension, to be discussed in IV.2.E, were also carried out at 25 °C using the Physica MCR301, along with a first generation Sentmanat extensional rheometer (SER). The stress relaxation tests after a stepwise shear, to be presented in section IV.2.C, were carried out at 30 °C using a second generation Advanced Rheometric expansion system (ARES-G2). The parallel plates had 8 mm diameter and its surfaces covered by sandpaper (grit 240 aluminum oxide, Virginia Abrasives, Petersburg, VA). To prevent wall slip, a thin layer of superglue (Loctite 498) was applied to glue the SBR160K onto the shearing sandpapers.

B. State of Entanglement after a Finite Amount of Strain Produced with $Wi_R \ll 1$. Under the condition of $Wi_R \ll 1$, the entanglement network should suffer little chain stretching according to the tube model. Thus, after an imposed strain produced with $Wi_R \ll 1$, the oriented network should simply relax toward its equilibrium state by molecular diffusion. In other words, the oriented state of chain entanglement should evolve monotonically toward the equilibrium. One effective method to probe the state of entanglement in the relaxing sample is to subject it to a fast startup shear at various stages of relaxation since the stress overshoot in response to startup shear can be used to delineate the state of chain entanglement.[81] Consider a protocol of a three-stage shear as depicted in Figure 6a. We apply this procedure to study the nonlinear responses of the PB solution.

When a second rate (higher than the first) is applied, the shear stress grows to a maximum value that is denoted as σ_{2max}. We first verified that the stress peak σ_{2max} associated with $\dot{\gamma}_2 = 15\ s^{-1}$ remained constant during relaxation upon a small stepwise strain of $\gamma = 0.3$, identical to the value obtained from a nonstrained sample. After a strain of $\gamma = 1.5$, produced with a rate of $\dot{\gamma}_1 = 0.25\ s^{-1}$ corresponding to $Wi_R \sim 0.1$, the state of chain entanglement during relaxation is probed by the application of a subsequent startup shear of $\dot{\gamma}_2 = 15\ s^{-1}$ in a series of discrete tests using the protocol of Figure 6a. Here the length of the second shear denoted by t_2 just needs to be long enough for the stress overshoot to emerge. In Figure 6b we see a nonmonotonic relation between σ_{2max} and the duration t_w of the stress relaxation period. Plotted in Figure 6b is also the stress growth and relaxation associated with the first shear produced at $\dot{\gamma}_1$. There are two features to note. First, the stepwise shear has produced a weaker entanglement state because the very first data point is appreciably lower than the points at long times (when the system has recovered the equilibrium state). Second, the emergence of a minimum in σ_{2max} vs t_w, though less than 10%, is consistent with the possibility that the entanglement network has suffered further

dx.doi.org/10.1021/ma300398x | Macromolecules 2013, 46, 3147–3159

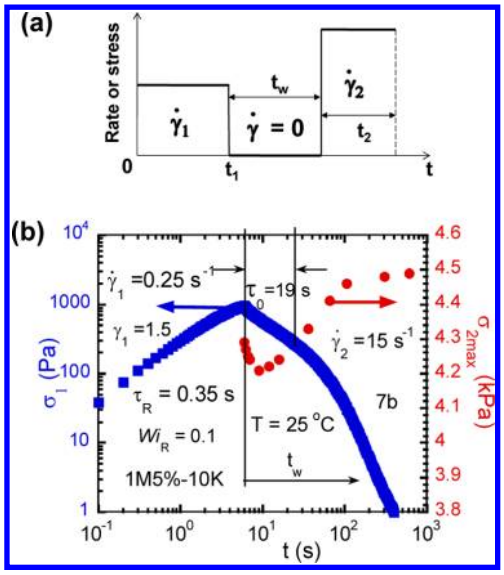

Figure 6. (a) Schematic depiction of the protocol used to probe changes in the state of chain entanglement during relaxation after an interrupted (at t_1) shear produced at $\dot\gamma_1$, where a second startup shear at $\dot\gamma_2$ is applied after a relaxation time t_w. (b) Stress relaxation behavior characterized by application of a startup shear at different stages of the relaxation (i.e., for different values of t_w) that produces a stress peak at σ_{2max}, where the squares indicate both the stress growth and decay as a function of time.

damage after cessation through the molecular elastic yielding mechanism discussed in subsection II.2.

C. Barrier to Chain Retraction upon Modest Deformation Made with $Wi_R > 1$. Linear response occurs in entangled polymers when external deformation is too low to affect the equilibrium state of chain entanglement. In other words, at a step strain of sufficiently low amplitude γ, stress relaxation dynamics should be independent of the value of the imposed step strain amplitude γ. Under such a condition, the state of entanglement should remain intact until the reptative process renews the network. When does a strained network undergo accelerated stress relaxation? At what value of γ does the entanglement network start to undergo faster stress relaxation? The tube model has definitive answers to these questions in its damping function. In particular, it asserts that chain retraction occurs about a Rouse time τ_R after shear cessation from a step strain of *any* amplitude.[82] Linear response ceases to be observed whenever a measurable acceleration of the stress relaxation emerges, as anticipated by eq 1a.

We carried out the following series of step shear experiments on the SBR160K melt. Figure 7a shows the normalized shear stress relaxation as a function of time for both $\gamma = 0.1$ and $\gamma = 0.7$. We define the relaxation modulus $G(t)$ as shown in Figure 7a because the strain took a finite time to stabilize at the prescribed value. The identical time dependence of the stress relaxation suggests that the entanglement state was intact after the step strain of $\gamma = 0.7$. In other words, up to a step strain of $\gamma = 0.7$, there exists a sufficiently high barrier against any faster relaxation of the strained network toward the equilibrium state. If we take the experimental data of $G(t,\gamma = 0.1)$ from the step strain of $\gamma = 0.1$ as the equilibrium relaxation modulus $G_{eq}(t)$, we can estimate the relaxation modulus $G(t, \gamma)$ from the tube model using eq 1a and α values in Figure 3. The tube model predicts a 13% difference as shown in Figure 7b that indicates how the barrier-free chain retraction has caused $G(t, \gamma = 0.7)$ to drop below $G_{eq}(t)$. The comparison between parts a and b of Figure 7 indicates that the tube-model-anticipated faster relaxation did not occur in experiment. In passing, we note that a previous SANS study[65] involving step extension to $\lambda = 1.7$ showed evidence of chain retraction. Unfortunately, there were no corresponding mechanical data to indicate whether such chain retraction produced any measurable stress drop.

It is probable[83] that the tube model could still be mended by introducing, for example, a barrier against chain retraction so as to reproduce the experimental data in Figure 7a. Erection of such a barrier may only be possible in some *ad hoc* manner within the tube model framework. At large step strains, the *ad hoc* barrier is overcome and the chain retraction can occur within the deformed tube. However, any such *ad hoc* modification necessarily degrades the formulation toward empirical modeling as in the case of the transient network models.[15−17]

D. Elastic Recovery after Startup Deformation. There is another way to demonstrate the existence of a finite barrier that resists any rapid rearrangement of chain entanglement. If a barrier-free chain retraction would take place for a step strain of

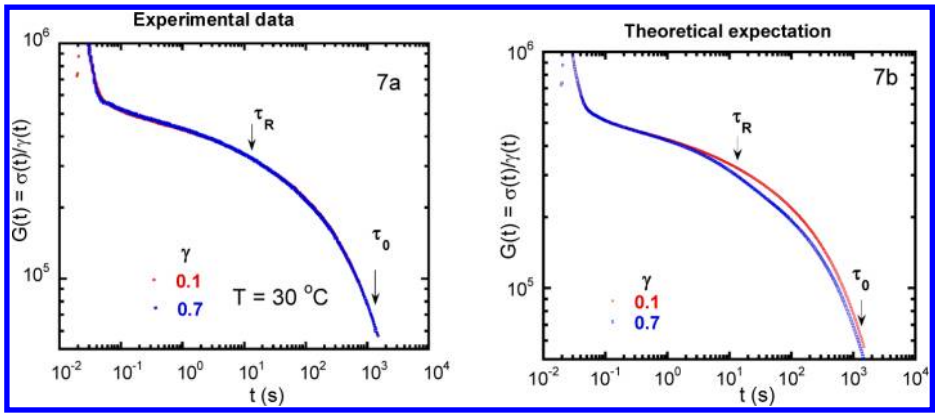

Figure 7. (a) Stress relaxation behavior from two discrete step strains of respective amplitudes $\gamma = 0.1$ and 0.7, which are completed within a period of 0.035 and 0.04 s respectively, much shorter than the Rouse time $\tau_R = 13$ s. Since the resulting shear stress after the step strain of $\gamma = 0.7$ deviates 4% downward from a perfectly linear relationship of $\sigma = G\gamma$, we have shifted the entire curve of $\gamma = 0.7$ upward by 4% to compare with $G(t, \gamma)$ measured from the step strain of $\gamma = 0.1$. (b) Taking $G(t, \gamma = 0.1)$ as $G_{eq}(t)$ in eq 1a, the relaxation modulus $G(t, \gamma = 0.7)$ can be estimated from the tube model that assumes the barrier-free chain retraction as described in eq 1a.

dx.doi.org/10.1021/ma300398x | *Macromolecules* 2013, 46, 3147−3159

γ < 1.0, the strained entanglement network may show signs of memory loss, i.e., reduce its ability to undergo elastic recovery. We performed a series of interrupted shear experiments at Wi_R > 1 with different amplitudes and set the strained sample stress-free after a given amount of time t_w. On the basis of the same sample as studied in Figure 6b, we show in Figure 8a the normalized strain recovery as a function of the strain amplitude γ, for six different waiting times t_w all longer than the Rouse time τ_R. The data in Figure 8a indicate that up to $\gamma \sim 1.0$ the entangled polymer solution did not lose its ability to undergo elastic recovery relative to that for $\gamma = 0.1$. Thus, the results of these elastic recovery tests are fully consistent with the preceding demonstration by stress relaxation measurements in Figure 7a: It appears that there exists a finite barrier against any accelerated return of the strained state to the equilibrium state. Figure 8b further demonstrates that the ability to undergo elastic recovery hardly decreases even when the sample was stress free after a relaxation time t_w 20 times the Rouse time τ_R.

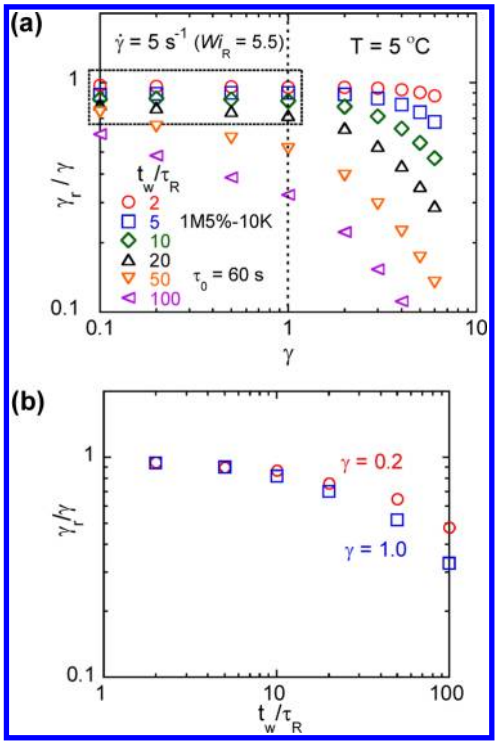

Figure 8. (a) Discrete elastic recovery tests for six waiting times t_w, measured relative to the Rouse time τ_R, after shear cessation from shear strain of amplitude γ produced with a rate corresponding to Wi_R = 5.5. Note that at T = 5 ° C, τ_R =1.1 s. Note that the first four sets of data, circled by the box, show little drop up to γ = 1. (b) The normalized degree of elastic recoil is plotted as a function of the waiting time t_w in the unit of the Rouse time, for two step strain amplitudes of 0.2 and 1.0. Up to t_w/τ_R = 20, there is little difference in their ability to undergo elastic recoil, between the sample step strained to 0.2 and to 1.0.

Finally, as discussed in III.1.C, the tube model does not expect the entanglement network to undergo any significant elastic recovery after a shear strain γ = 2 produced with $Wi_R \ll 1$. Using the same sample as studied in Figure 6b and 8a,b, we conducted a combination of startup shear and elastic recovery experiments at different stages for various shear rates including $\dot{\gamma}$ = 0.3 s^{-1}. Figure 9a shows the stress vs time data for four rates ranging from 0.3 to 10 s^{-1}. To better understand the origin of the stress overshoot, we evaluate the degree of elastic recovery both before and after the shear stress maximum at the shear strain of γ_{max}. Figure 9b summarizes how the ability to undergo elastic recovery varies as a function of the imposed strain γ, normalized by γ_{max}.

Figure 9b reveals some interesting information. (a) The entanglement network makes complete elastic recovery for Wi_R as low as 0.1 up to γ_{max} where the stress shows a maximum, i.e., at $t_{max} \sim 20\tau_R$. Thus, even this shearing condition of Wi_R = 0.1 amounts to producing significant affine deformation, contrary to the picture given by the tube model that the system should be undergo nonaffine deformation from τ_R to $20\tau_R$. (b) The point of the stress maximum is significant, separating recoverable deformation from irrecoverable deformation. Thus, Figure 9b represents systematic evidence supporting the phenomenological notion of macroscopic yielding at the stress overshoot.

E. Yielding after Maximum in σ_{engr} in Startup Extension. The Doi–Edwards tube model predicts the tensile force or engineering stress σ_{engr} would show a maximum around λ_{max} = 2.36 because the Cauchy stress $\sigma = \sigma_{engr}\lambda$ would level off upon saturation of the chain orientation in absence of chain stretching (i.e., for $Wi_R \ll 1$). According to the tube model, σ_{engr} declines when the chain orientation cannot further increase and less chains are involved in producing the stress as the cross-sectional area shrinks, as illustrated in Figure 5a. We performed a combination of startup uniaxial extension and elastic recovery experiments to explore the nature of the maximum in σ_{engr} using a second SBR241K melt.

At a Hencky rate $\dot{\varepsilon}$ = 1.0 s^{-1}, Wi_R = 0.12 ≪ 1, we show in Figure 10 that the elastic recovery, as measured by the degree

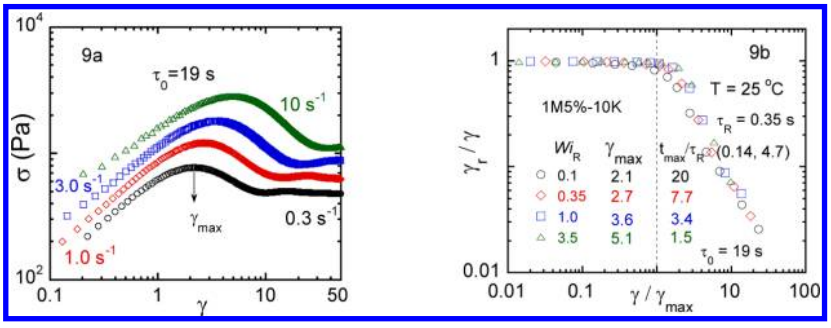

Figure 9. (a) Shear stress vs the imposed strain $\gamma = \dot{\gamma}t$, showing stress overshoot in each of the four applied rates. Note that for the first rate of 0.3 s^{-1} the stress at the strain γ = 9.9 = 4.7γ_{max} is 63% of the peak value. (b) Recoverable strain γ_r as a function of imposed strain γ, either before or beyond the stress maximum that occurs at γ_{max}, involving four values of $\dot{\gamma}$.

dx.doi.org/10.1021/ma300398x | Macromolecules 2013, 46, 3147–3159

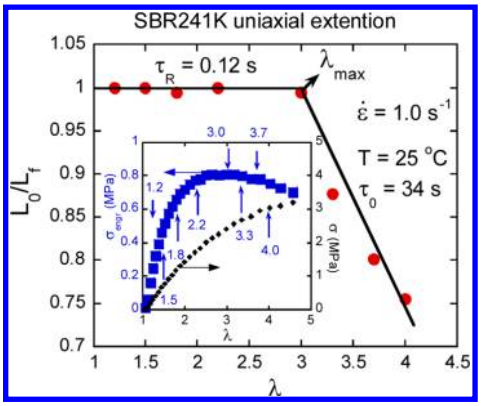

Figure 10. Ratio of the initial specimen length L_0 to the final recovered length L_f of SBR241K melt after it has been stretched to the various values of the stretching ratio λ = 1.2, 1.5, 1.8, 2.2, 3.0 (λ_{max}), 3.3, 3.7, and 4 respectively. The inset shows the raw data of stress vs strain (σ_{engr} vs λ) at the Hencky rate of 1.0 s^{-1}, corresponding to $Wi \ll 1$, as well as the eight positions along the curve when the extension is terminated (i.e., setting the stretched specimen stress free) to allow elastic recovery. Note that the Cauchy stress (diamonds) $\sigma = \lambda\sigma_{engr}$ shows only monotonic rise with λ.

of return to the original length L_0, is nearly complete when the stretched specimen is let go before the peak of σ_{engr}. The inset of Figure 10 indicates the corresponding rheometric information before and after the yield point at $\lambda_{max} \simeq 3.0$, where the Cauchy stress $\sigma = \sigma_{engr}\lambda$ monotonically grows in the explored range of the stretching ratio λ. It is clear that the maximum of σ_{engr} is a special moment during the startup extension. Beyond λ_{max}, the recovered sample length L_f is appreciably higher than L_0, indicating that the entanglement network suffered irrecoverable changes. The DE tube model does not explicitly explore[78] the significance associated with the peak of σ_{engr}, which signifies yielding. It remains to be seen how remedies can be made within the framework of the tube model to provide a realistic molecular picture for the observed yielding of entangled melts during startup uniaxial extension.

V. SUMMARY

Four decades ago, de Gennes' idea of reptation[1] revolutionized the study of chain dynamics in entangled polymeric liquids, and subsequently the Doi–Edwards tube model[2] illuminated a new direction of research in polymer rheology. Because of these theoretical advances, we have achieved an unprecedented level of understanding, concerning linear viscoelastic properties[24,25] of linear and long-chain-branched polymers. It has been widely known that the tube model also attempted to describe many of the nonlinear rheological characteristics.[26,45,65,69−72] However, the recent particle-tracking velocimetric observations of various strain localization phenomena such as shear banding[50,51] and nonquiescent relaxation[39,40] have caused us to search for an alternative theoretical depiction.

In this paper, after briefly discussing what we may expect from large deformation of entangled polymers, we first described in section II the construction of the tube model and then outlined an alternative conceptual framework. After introducing the basic features and pictures associated with the tube model in section III, we reviewed two major classes of previously reported strain localization phenomena in the experimental section IV before delineating four new experiments carried out in absence of any inhomogeneity and edge fracture. On the basis of these new results, we suggest that the tube theory might have oversimplified the treatment of the heterogeneous intermolecular (excluded volume) interactions in terms of a smooth static tube. It remains to be seen whether any new mending within the tube-model framework can actually elucidate the phenomena, i.e., nonmonotonic changes of the stress peak from the second applied shear during relaxation after the first slow shear (cf. Figure 6b) as well as lack of nonlinear damping of the relaxation modulus for a moderate strain (cf. Figure 7a), both of which are consistent with our scenarios of molecular elastic "yielding" and presence of entropic barrier against chain retraction.

Either during startup shear with $Wi_R \ll 1$ or after step strain, the dominant contribution to the shear stress is chain orientation in the tube model, whereas in our alternative picture the shear stress is due to the overall chain deformation including stretching before the point of force imbalance. Thus, the stress overshoot is just attributed to chain orientation in the tube model and chain disentanglement accelerated by the intrachain elastic retraction in the alternative picture. Similarly, the strain softening observed under step strain is again due to the chain orientation in the tube model, but is a consequence of elastic yielding and breakdown of the entanglement network in the alternative picture.

Since no revision of the tube model has been made to include the new ingredients discussed in this work, it is too early to conclude that the tube model cannot be further improved to quantify the rheometric measurements such as those presented here. It also remains to be seen whether a new analytical theory will emerge to deal with the nearly intractable challenge to account for the interchain uncrossability that produces chain entanglement. It is encouraging to mention that by explicitly accounting for binary chain uncrossibility, Sussman and Schweizer have recently developed a first principles microscopic theory for the transverse tube confinement potential of topologically entangled solutions of rod-like polymers.[84] According to their theory, the tube-like confining potential has a finite barrier. Specifically, they predict that the maximum confining force to keep a polymer in the tube is of the form of k_BT/l_{ent} and suggest that there is indeed finite cohesion. They also show that the presence of sufficient stress can result in molecular yielding, i.e., chain delocalization out of the confining tube.[85,86] These theoretical results, though obtained for rods but not for flexible chains that are examined in the present study, are consistent with the conceptual picture summarized in Figure 2. More recently, they have qualitatively extended their microscopic dynamical theory for the transverse confinement of infinitely thin rigid rods to study topologically entangled melts of flexible polymer chains.[87]

Molecular dynamics computer simulations are expected to play a critical role to elucidate the molecular pictures behind the various macroscopic observations and identify necessary ingredients to include in a more realistic theoretical description of nonlinear responses of entangled polymers to large fast deformation. In particular, they could elucidate whether lateral constraints are still present during the accelerated stress decline involving either startup deformation or interrupted deformation, and whether chains stretch considerably upon startup deformation even for $Wi_R < 1$. Such simulations will be different from those that have been performed[88] so far based on a static characterization of chain entanglement via primitive path analyses.[89−91] Hopefully, the future experiments and molecular

dynamics simulations can thoroughly test the ideas of finite cohesion, force imbalance, and chain disentanglement.

AUTHOR INFORMATION

Corresponding Author

*E-mail: (S.-Q.W.) swang@uakron.edu.

Notes

The authors declare no competing financial interest.

ACKNOWLEDGMENTS

The present work is supported, in part, by grants from the US National Science Foundation (DMR-0821697, CMMI-0926522, and DMR-1105135). S.-Q.W. communicated with K. Schweizer in numerous emails that inspired him to examine the relationship between the emerging phenomenology and the tube model. SQW greatly appreciates the interest from A. Gent to read the first version of the manuscript, as well as helpful comments on the manuscript from M. Cates, K. Schweizer, H. Watanabe, J. Schieber and R. Graham. Most importantly, the reviewers' comments helped improve the presentation in significant ways. Finally, we are grateful to Dr. R. Weiss who made the ARES-G2 rheometer available for our experiment.

DEDICATION

†In commemoration of the 40th anniversary of de Gennes' publication of the celebrated reptation idea.

REFERENCES

(1) de Gennes, P. G. *J. Chem. Phys.* **1971**, *55*, 572.

(2) Doi, M.; Edwards, S. F. *J. Chem. Soc., Faraday Trans. II* **1978**, *74*, 1789.

(3) Doi, M.; Edwards, S. F. *J. Chem. Soc., Faraday Trans. II* **1978**, *74*, 1802.

(4) Doi, M.; Edwards, S. F. *J. Chem. Soc., Faraday Trans. II* **1978**, *74*, 1818.

(5) Doi, M.; Edwards, S. F. *J. Chem. Soc., Faraday Trans. II* **1979**, *75*, 38.

(6) Edwards, S. F. *Proc. Phys. Soc.* **1967**, *92*, 9; *Polymer* **1977**, *9*, 140.

(7) Astarita, G.; Marrucci, G. *Principles of Non-Newtonian Fluid Mechanics*; McGraw-Hill Inc.: Columbus, OH, 1974.

(8) Schowalter, W. R. *Mechanics of Non-Newtonian Fluids*; Pergamon Press: Oxford, U.K., 1978.

(9) Bird, R. B.; Armstrong, R. C. ; Hassager, O. *Dynamics of Polymeric Liquids*; Wiley: New York, 1987.

(10) Larson, R. G. *Constitutive equations for polymer melts and solutions*; Butterworths: London, 1988.

(11) Bird, R. B.; Wiest, J. M. *Ann. Rev. Fluid Mech.* **1995**, *27*, 169.

(12) Kaye, A. *Non-Newtonian Flow in Incompressible Fluids*; College of Aeronautics Press: Cranford, U.K, 1962.

(13) Bernstein, B.; Kearsley, E. A.; Zapas, L. J. *Trans. Soc. Rheol.* **1963**, *7*, 391.

(14) Guth, E.; Mark, H. F. *Monatsh. Chem.* **1934**, *65*, 93.

(15) Green, M. S.; Tobolsky, A. V. *J. Chem. Phys.* **1946**, *14*, 80.

(16) Yamamoto, M. *J. Phys. Soc. Jpn.* **1956**, *11*, 413; **1957**, *12*, 1148; **1958**, *13*, 1200.

(17) Lodge, A. S. *Rheol. Acta* **1968**, *7*, 379.

(18) Lodge, A. S. *Elastic Liquids*; Academic Press: London, 1964.

(19) Rault. *J. C. R. Acad. Sci. Paris, Ser. II* **1985**, *300*, 433. Rault, J. *J. Non-Newton. Fluid Mech.* **1987**, *23*, 229.

(20) Heymans, N. *J. Mater. Sci.* **1986**, *21*, 1919.

(21) Lin, Y.-H. *Macromolecules* **1987**, *20*, 3080.

(22) Kavassalis, T. A.; Noolandi, J. *Phys. Rev. Lett.* **1987**, *59*, 2674.

(23) Lodge, A. S. *Rheol. Acta* **1989**, *28*, 351.

(24) Watanabe, H. *Prog. Polym. Sci.* **1999**, *24*, 1253.

(25) McLeish, T. C. B. *Adv. Phys.* **2002**, *51*, 1379.

(26) Graham, R. S.; Likhtman, A. E.; McLeish, T. C. B.; Milner, S. T. *J. Rheol.* **2003**, *47*, 1171.

(27) Our network picture is rather different from the transient network models where upon a large stepwise deformation a sufficient elastic retraction within a Gaussian strand has never been perceived to lead to a breakdown of the network.

(28) The chain uncrossability, as the origin of chain entanglement, stems from excluded volume interactions (EVI). However, the EVI alone are insufficient to ensure "uncrossability" as defined in this work: chain connectivity and sufficient chain length are necessary. In other words, as well recognized, chain entanglement arises only when the chain length exceeds a critical value. When the chains are short, uncrossability is ineffective in producing any slowing down of chain dynamics. Consequently, no entanglement occurs. According to the packing model, entanglement arises when chains are long enough so that in the pervaded volume of a test chain there are a sufficient number of other chains sharing the same space. Uncrossability only provides the constraint and has been successfully modeled by perceiving a test chain in a tube. In absence of fast and large external deformation, the uncrossability of one chain does not exert directional force on other chains. Therefore, the idea of reptation in a tube is an excellent simplification to treat chain dynamics in quiescence. When fast and large external deformation is present, the uncrossability plays an active role: it gives birth to the IGF.

(29) Wang, S. Q.; Ravincdranath, S.; Wang, Y. Y.; Boukany, P. E. *J. Chem. Phys.* **2007**, *127*, 064903.

(30) Wang, Y. Y.; Wang, S. Q. *J. Rheol.* **2009**, *53*, 1389.

(31) Ravindranath, S.; Wang, S. Q. *J. Rheol.* **2008**, *52*, 681. Boukany, P. E.; Wang, S. Q.; Wang, X. R. *J. Rheol.* **2009**, *53*, 617.

(32) Zhu, X. Y.; Wang, S. Q. *J. Rheol.* **2013**, *57*, 223.

(33) Matsuoka, S. *Relaxation Phenomena in Polymers*; Hanser Publishers: Munich, Germany, 1992.

(34) Lee, H.-N.; Paeng, K.; Swallen, S. F.; Ediger, M. D. *Science* **2009**, 231.

(35) Lindstrom, S. B.; Kodger, T E.; Weitz, D A. *Phys. Rev. Lett.* **2011**, *106*, 248303.

(36) Li, X.; Wang, S. Q. *Rheol. Acta* **2010**, *49*, 89.

(37) Wang, S. Q.; Ravindranath, S.; Boukany, P. E. *Macromolecules* **2011**, *44*, 183.

(38) Ravindranath, S.; Wang, S. Q.; Olechnowicz, M.; Chavan, V. S.; Quirk, R. P. *Rheol. Acta* **2011**, *50*, 97.

(39) Wang, S. Q.; Ravindranath, S.; Boukany, P. E.; Olechnowicz, M.; Quirk, R. P.; Halasa, A. *Phys. Rev. Lett.* **2006**, *97*, 187801. Ravindranath, S.; Wang, S. Q. *Macromolecules* **2007**, *40*, 8031.

(40) Boukany, P. E.; Wang, S. Q.; Wang, X. R. *Macromolecules* **2009**, *42*, 6261.

(41) In this zeroth order picture, we regard the topological structure of an entangled polymer to be statistically uniform at all levels down to the scale of entanglement spacing. For the sake of conceptual simplicity, we have discussed the force imbalance as a single molecular event that occurs at the yield point corresponding to the force maximum. In reality, dynamic yielding, i.e., the transition from solid-like to liquid-like due to reduced entanglement occurs when strain softening is observed upon startup deformation well before the global yield point at the force maximum. We have also pointed out recently that there may be a spectrum of entanglement strength distribution, implying occurrence of sequential disentanglement: Wang, Y. Y.; Wang, S. Q. *Macromolecules* **2011**, *44*, 5427. There have been suggestions in the literature that the polymer entanglement dynamics may be spatially inhomogeneous. There is even speculation that the chain entanglement is more of enthalpic origin than topological, i.e., there could be strongly interacting domains in polymer melts responsible for the elastic network-like mechanical responses, at temperatures well above the glass transition temperature. See Ibar, J. P. *J. Macromol. Sci. B* **2010**, *49*, 1148; **2009**, *48*, 1143; *J. Macromol. Sci. Rev. Macromol. Chem. Phys.* **1997**, *C37*, 389 However, any discussion of other mechanisms for chain entanglement is beyond the scope of this work due to the limited space..

(42) Marrucci, G.; Grizzuti, N. *J. Rheol.* **1982**, *27*, 433.

(43) Wang, Y. Y.; Boukany, P. E.; Wang, S. Q.; Wang, X. R. *Phys. Rev.* **2007**, *99*, 237801.
(44) Wang, Y. Y.; Wang, S. Q. *J. Rheol.* **2008**, *52*, 1275.
(45) Doi, M. *J. Polym. Sci., Part B: Polym. Phys.* **1980**, *18*, 1005 Theoretically, "step strain" is understood to involve imposition of a finite external strain in an instant. In experiment, any magnitude of step strain would take a finite time to realize. If the time required by a rheometer to produce the desired strain amplitude is negligibly short relative to the material relaxation times, then the test can be regarded as a step strain..
(46) Doi, M.; Edwards, S. F. *The Theory of Polymer Dynamics*; Oxford University Press: Oxford, U.K., 1986.
(47) Olmsted, P. D.; Radulescu, O.; Lu, C. Y. D. *J. Rheol.* **2000**, *44*, 257.
(48) Olmsted, P. D. *Rheol. Acta* **2008**, *47*, 283.
(49) Adams, J. M.; Fielding, S. M.; Olmsted, P. D. *J. Rheol.* **2011**, *55*, 1007.
(50) Tapadia, P.; Wang, S. Q. *Phys. Rev. Lett.* **2006**, *96*, 016001.
(51) Boukany, P. E.; Wang, S. Q. *J. Rheol.* **2007**, *51*, 217;Ravindranath, S.; Wang, S. Q. *J. Rheol.* **2008**, *52*, 957.
(52) Graessley, W. W.; Prentice, J. S. *J. Polym. Sci., Part A2: Polym. Phys.* **1968**, *6*, 1887.
(53) Marrucci, G. *J. Non-Newtonian Fluid Mech.* **1996**, *62*, 279.
(54) Likhtman, A. E.; Milner, S. T.; McLeish, T. C. B. *Phys. Rev. Lett.* **2000**, *85*, 4550.
(55) Milner, S. T.; McLeish, T. C. B.; Likhtman, A. E. *J. Rheol.* **2001**, *45*, 539.
(56) Auhl, D.; Ramirez, J.; Likhtman, A. E.; Chambon, P.; Fernyhough, C. *J. Rheol.* **2008**, *52*, 801.
(57) Pearson, D. S.; Kiss, A. D.; Fetters, L. J.; Doi, M. *J. Rheol.* **1989**, *33*, 517.
(58) Menezes, E. V.; Graessley, W. W. *J. Polym. Sci., Polym. Phys. Ed.* **1982**, *20*, 1817.
(59) Osaki, K.; Inoue, T.; Isomura, T. *J. Polym. Sci., Part B: Polym. Phys.* **2000**, *38*, 1917.
(60) For the linear response regime, recent computer simulation works have been carried out to support the foundation of the tube model. See: Everaers, R.; Sukumaran, S. K.; Grest, G. S.; Svaneborg, C.; Sivasubramanian, A.; Kremer, K. *Science* **2004**, *303*, 823. Tzoumanekas, C.; Theodorou, D. N. *Macromolecules* **2006**, *39*, 4592 On the basis of a primitive path analysis, the tube diameter was deduced..
(61) As a foundational issue, whether the stress tensor can be evaluated solely based on bonded forces has been raised long ago by Fixman, M. *J. Chem. Phys.* **1991**, *95*, 1410. and Gao, J.; Weiner, J. H. *Macromolecules* **1991**, *24*, 5179. and restated more recently in Likhtman, A. E. *J. Non-Newtonian Fluid Mech.* **2009**, *157*, 158 An ad hoc way to remedy this situation is to add a viscous stress to represent the frictional intermolecular interactions. In steady flow the nature of stress is necessarily entirely viscous, originating from intermolecular interactions. At rates higher than $Wi_R = (M/M_e)^2$, the stress is no longer dependent on the molecular weight M. Conversely, at lower rates, the viscous stress does still depend on the chain length. In contrast, the tube model assumes that even the steady stress is entropic in origin.
(62) Larson, R. G. *J. Polym. Sci., Part B: Polym. Phys* **2007**, *45*, 3240.
(63) The potential difficulty facing the tube model has been mentioned in Graessley, W. W. *Polymer Liquids & Networks: Dynamics and Rheology*; Garland Science: New York, 2008; p 548: "It seems in fact possible that rapid and sustained deformations, those responsible for nonlinear response, alter the liquid structure in ways that are not intrinsic to the (tube) theory, thus requiring new mechanisms to be added."
(64) Wang, S. Q. *J. Polym. Sci., Part B: Polym. Phys.* **2008**, *46*, 2660.
(65) For example, SANS measurements were carried out to show the chain retraction indeed occurs when the imposed rate of deformation is higher than the Rouse relaxation rate. See: Blanchard, A.; et al. *Phys. Rev. Lett.* **2005**, *95*, 166001 The experiment was not designed to show whether chain retraction would occur at lower imposed strain and whether chain stretching would also take place for $Wi_R < 1$..
(66) Boukany, P. E.; Wang, S. Q. *Macromolecules* **2010**, *43*, 6950. which was based on entangled DNA solutions. Cheng, S. W.; Wang, S. Q. *J. Rheol.* **2012**, *56*, 1413 which was based on entangled polybutadiene solutions..
(67) Adams, J. M.; Fielding, S. M.; Olmsted, P. D. *J. Rheol.* **2011**, *55*, 1007 This work attempted to depict transient shear banding using a simplified version of the most comprehensive tube model (ref 26.). In absence of a constitutive non-monotonicity, shear inhomogeneity could arise in their calculations only if the system experiences a shear stress gradient along the velocity gradient direction. Although one cannot claim that a perfectly constant stress distribution can be established cross the sample thickness in a simple shear apparatus, one cannot rule out either that the strain localization is not due to a genuine cohesive breakdown of the entanglement network. Whether there is strain localization or not depends intimately on whether or not the disentangled state is sufficiently different from the entanglement state (cf. refs 37 and 38), and on how the external shearing is imposed (cf. ref 66).
(68) Often more information can be obtained if the rheometer applies a startup shear at a given rate and interrupts it within a certain amount of time to attain a prescribed level of strain. Throughout this paper, we adopt a generalization of the concept "step strain" and use the phrase to refer to any interrupted startup deformation involving a prescribed rate of deformation.
(69) Osaki, K. *Rheol. Acta* **1993**, *32*, 429.
(70) Osaki, K.; Nishizawa, K.; Kurata, M. *Macromolecules* **1982**, *15*, 1068.
(71) Osaki, K.; Kurata, M. *Macromolecules* **1980**, *13*, 671.
(72) Larson, R. G.; Khan, S. A.; Raju, V. R. *J. Rheol.* **1988**, *32*, 145. Sanchez-Reyes, J.; Archer, L. A. *Macromolecules* **2002**, *35*, 5194.
(73) For a step strain with amplitude $\gamma > 1$, some previous experiments reported that the "time-strain separability" occurs at times significantly longer than τ_R: Inoue, T.; Yamashita, Y.; Osaki, K. *Macromolecules* **2002**, *35*, 1770. and Archer, L. A.; Sanchez-Reyes, J.; Juliani. *Macromolecules* **2002**, *35*, 10216. A variation of the tube theory Mhetar, V.; Archer, L. A. *J. Non-Newtonian Fluid Mech.* **1999**, *81*, 71 indicates this separablility should occur at τ_0, not τ_R. It also suggests that the barrier-free chain retraction may not completely restore the contour length. Since such modeling shares the same foundation as the tube model, it is not fundamentally different from the other tube models..
(74) Vrentas, C. M.; Graessley, W. W. *J. Rheol.* **1982**, *26*, 359.
(75) Boukany, P. E.; Wang, S. Q. *Macromolecules* **2009**, *42*, 2222.
(76) Boukany, P. E.; Wang, S. Q. *J. Rheol.* **2006**, *50*, 641.
(77) Adams, J. M.; Olmsted, P. D. *Phys. Rev. Lett.* **2009**, *102*, 067801; *Phys. Rev. Lett.* **2009**, *103*, 219802. Wang, S. Q. *Phys. Rev. Lett.* **2009**, *103*, 219801.
(78) In ref 5. the idea of the Considère criterion was used to suggest occurrence of nonuniform extension, confusing the relation of cause and effect: the experimentally observed engineering stress maximum is the consequence of force imbalance, leading to massive chain disentanglement, rather than the cause of any subsequent shear yielding (that can initialize unstable necking). Moreover, the Considère criterion does not encompass any microscopic physics about how and why nonuniform extension may occur after the maximum. Our experiment in the subsequent Figure 10 shows that the engineering stress maximum signifies yielding, i.e., a transition from elastic to irrecoverable deformation.
(79) Whether wall slip, shear banding and nonquiescent relaxation would occur depend on a specific material parameter known as the extrapolation length b that can be reduced sufficiently by employing entangled polymeric solvents. See refs 37 and 38 for more detailed discussion about the strategy implemented to suppress strain localization.
(80) The Rouse time can be estimated in two ways. We found similar values: According to the Osaki formula of $\tau_{R\eta} = (6M_w\eta/\pi^2\rho RT)(M_c/M_w)^{2.4}$ where M_c is chosen to be $2M_e$, we have 13.5 s. When evaluating

from the high frequency data according to $\tau_{R\omega} = (aM/1.111\rho RT)^2$ where a is the prefactor for the scaling behavior of the storage modulus $G' = a\omega^{1/2}$, we get 13.2 s. See a discussion of the two formulas in ref 59.
(81) Robertson, C. G.; Warren, S.; Plazek, D. J.; Roland, C. M. *Macromolecules* **2004**, *37*, 10018.
(82) Blanchard, A.; et al. *Phys. Rev. Lett.* **2005**, *95*, 166001 This study involved large stepwise extension at rates satisfying $Wi_R > 1$ and reported evidence of chain retraction. But it did not explore whether there could be a critical strain below which chain retraction would not occur on the Rouse time scale..
(83) Private communication with M. Cates.
(84) Sussman, D. M.; Schweizer, K. S. *Phys. Rev. Lett.* **2011**, *107*, 078102.
(85) Sussman, D. M.; Schweizer, K. S. *J. Chem. Phys.* **2011**, *135*, 131104.
(86) Sussman, D. M.; Schweizer, K. S. *Macromolecules* **2012**, *45*, 3270.
(87) Sussman, D. M.; Schweizer, K. S. *Phys. Rev. Lett.* **2012**, *109*, 168306.
(88) Baig, C.; Mavrantzas, V. G.; Kroger, M. *Macromolecules* **2010**, *43*, 6886.
(89) Everaers, R.; Sukumaran, S. K.; Grest, G. S.; Svaneborg, C.; Sivasubramanian, A.; Kremer, K. *Science* **2004**, *303*, 823.
(90) Tzoumanekas, C.; Theodorou, D. N. *Macromolecules* **2006**, *39*, 4592−4604.
(91) Foteinopoulou, K.; Karayiannis, N. C.; Mavrantzas, V. G.; Kröger, M. *Macromolecules* **2006**, *39*, 4207.